

Dynamics of the Hole-Capture Processes in Biphenyl and Poly(4-vinylbiphenyl): A Direct ab Initio Trajectory Study

Hiroto Tachikawa*

Division of Molecular Chemistry, Graduate School of Engineering, Hokkaido University, Sapporo 060-8628, Japan

Hiroshi Kawabata

Venture Business Laboratory, Osaka University, Suita, Osaka 565-0871, Japan

Received: June 28, 2002; In Final Form: November 21, 2002

Direct ab initio trajectory calculations have been applied to the ionization (i.e., hole-capture) processes of biphenyl (Bp) in order to shed light on hole-capture processes of Bp and poly(4-vinylbiphenyl) (PVB). The static ab initio calculations at several levels of theory showed that the neutral Bp has a nonplanar structure with a twist angle between benzene rings in the range $\phi = 38\text{--}50^\circ$. The potential energy curve for the twist rotation of benzene rings was shallow for Bp. This twist angle was changed to $18\text{--}21^\circ$ in biphenyl cation (Bp^+), which has a more planar structure and a more tight potential shape than those of Bp. Full dimensional direct ab initio trajectory calculations showed that the structure of Bp is spontaneously changed after the ionization: the nonplanar structure was changed to planar one after 120 fs, and then the twist angle vibrated between -40° and $+40^\circ$ with a time period of about 500 fs. The C–C bond distance in the connection site between two benzene rings was immediately shortened after the hole capture of Bp, and it vibrated in the range 1.375–1.481 Å. Direct PM3 dynamics calculations for the model compound composed of two-monomer units of PVB indicated that a hole is localized on one of the biphenyl groups at time zero, and then it is delocalized over the two side-groups after the structural relaxation. The mechanism of hole capture in Bp and in PVB was discussed on the basis of theoretical results.

1. Introduction

Biphenyl (Bp) and its halogen derivatives have been widely used as one of the electron and hole scavengers in several reaction systems^{1,2} because Bp has a large cross section for acceptor of low energy electron (electron affinity: $E_a = 0.13$ eV)³ and low ionization potential ($I_p = 8.34$ eV in gas phase).⁴ These reactions are schematically expressed by



Reaction I is a hole transfer reaction from a positive charged molecule A^+ to Bp, while reaction II is an electron capture process of Bp, where A means an arbitrary molecule. In the S_0 state of Bp, the two benzene rings are twisted by about 45° in the gas phase^{5–7} but are thought to be coplanar in the anion, cation, or excited state.^{8,9} This implies that the structure of Bp would be largely deformed by electron and hole captures and energy transfer.

Also, the aromatic group in polymer (e.g., biphenyl, phenyl, and triphenylamine) is known as a good side-chain possessing ability of electron and hole scavengers and that of charge-transfers along polymer chain.^{10,11} These polymers have been utilized as electro-luminescence (EL) materials, organic light emission diode (LED) devices and organic hole transport materials^{12–14}. A recent experiment has shown that the EL efficiency for the polymer having aromatic groups as side chains is significantly larger than that of monomers in polymer film.

For example, in the case of poly(4-vinyltriphenylamine), which is a polymer with pendant triphenylamine groups in a hydrocarbon backbone, quantum efficiency of the devices is 0.45–1.0% in the polymer, which is significantly larger than that of the devices composed of its monomer (1.3×10^{-3} %). This implies that the aromatic group in polymer has a higher performance than the monomer crystallized in polymer film because of the effect of polymerization. However, the details of mechanism are not clearly understood.

From a recent density functional theory (DFT) calculation,¹⁵ it has been shown that the twist angle ϕ for Bp, Bp^+ , and Bp^- are calculated to be 40.1° , 18.9° , and 0.0° at B3LYP/6-311+G-(2d,2p) level of theory, respectively. Ionization potential and electron affinity were calculated to be 7.86 and 0.03 eV, respectively. The electronic spectra of the cation and anion of biphenyl were studied using multiconfiguration second-order perturbation (CASPT2) theory. For both ions, two main transitions were predicted.¹⁶ Thus, static properties for ionic species of Bp have been investigated extensively from theoretical calculations and experiments. However, the dynamics for hole and electron capture processes are not clearly understood. In particular, hole localization and hole transport mechanism in polymer are still unclear.

In the present study, the ionization dynamics of Bp were investigated by means of direct ab initio trajectory method¹⁷ in order to shed light on the initial stage of the hole capture in Bp and in poly(4-vinylbiphenyl) (denoted by PVB), which is a polymer with pendant biphenyl group on a hydrocarbon backbone. The hole-capture process of Bp is

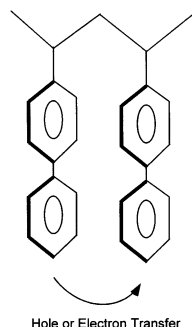
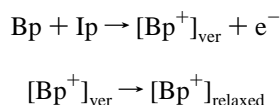


Figure 1. Schematic illustration of hole and electron transfers along the side-chains in polymer. Two monomer units having two pendant biphenyl groups in poly(4-vinylbiphenyl) are only illustrated.

schematically expressed by



where $[\text{Bp}^+]_{\text{ver}}$ is the biphenyl cation at the vertical ionization point of Bp, $[\text{Bp}^+]_{\text{relaxed}}$ is the fully relaxed biphenyl cation, and Ip is a vertical ionization potential of Bp. In the case of PVB, the energy relaxation process is expected to be much different from the isolated Bp^+ . Therefore, the dynamics in Bp and PVB would be different from each other. In the present study, we also focus our attention on this point.

Figure 1 shows two monomer units of PVB and a schematic illustration for hole (or electron) transfer in PVB. It is known that PVB has an ability as electron and hole-capture polymer,¹⁰ and these species can be transferred along the side chain. In this work, we calculated the hole-capture dynamics in two unit model of PVB as well as that of Bp. The process is important as an initial elementary step of polymer induced by ionizing radiation and photoirradiation.

2. Computational Methods

Classical trajectory calculations, in general, are performed on an analytically fitted potential energy surface (PES).^{18,19} However, it is not appropriate to predetermine the reaction surfaces of the present systems due to the large number of degrees of freedom ($3N - 6 = 102$ for Bp and $3N - 6 = 210$ for the model compound of PVB, where N is number of atoms in the system). Therefore, in the present study, we applied direct ab initio trajectory calculation with all degrees of freedom to the ionization dynamics of Bp. In the procedure, the energy gradients for all atoms of molecule are full-dimensionally calculated at each time step, and then the trajectory propagates.

Direct ab initio trajectory calculations^{20–22} were carried out at the UHF/3-21G(d) level of theory throughout. On the assumption of vertical ionization of Bp, trajectories on the ground-state PES of Bp^+ were run. The trajectory calculations of Bp^+ were performed under a constant total energy condition. The velocities of atoms at the starting point were assumed to be zero (i.e. momentum vector of each atom is zero). The equations of motion for n atoms in a molecule are given by

$$\frac{dQ_j}{dt} = \frac{\partial H}{\partial P_j}$$

$$\frac{\partial P_j}{\partial t} = \frac{\partial H}{\partial Q_j} = \frac{\partial U}{\partial Q_j} \quad (1)$$

where $j = 1 - 3N$, H is the classical Hamiltonian, Q_j is the Cartesian coordinate of j th mode, and P_j its conjugated momentum. These equations were numerically solved using the Runge–Kutta method. No symmetry restriction was applied to the calculation of the gradients. The time-step size chosen was 0.10 fs, and a total of 10000 steps were calculated for each dynamic calculation. The drift of the total energy is confirmed to be less than $1 \times 10^{-3} \%$ throughout at all steps in the trajectory. The momentum of the center of mass and the angular momentum are assumed to be zero. Static ab initio MO calculations were carried out using Gaussian 98 program package at several levels of theory with several basis sets²³ in order to obtain more accurate energetics.

For the hole capture in PVB, a model compound constructed from two monomer units of PVB was employed. This fragment was terminated by a methyl group and a hydrogen atom. Two biphenyl groups are connected to a normal pentane as pendant group. The structure of the model of PVB has no symmetry and deviates from the C_s structure. This is due to the fact that the phenyl rings are parallel to each other and each phenyl group is twisted from the molecular axis of polymer chain. The direct trajectory calculations were carried out at the semiempirical PM3 level of theory. Note that CPU time for one trajectory of Bp^+ was 2 weeks using a Pentium IV processor (2.5 GHz clock time and 1.0 GHz memory), and that of model PVB was about 10 min for one trajectory.

3. Results

I. Hole-Capture Dynamics of Biphenyl. *A. Structures of Biphenyl Neutral and Cation.* The structures of biphenyl neutral (Bp) and biphenyl cation (Bp^+) were fully optimized at several levels of theory. The dihedral angles between two benzene rings (twist rotation angle ϕ) and the C–C bond distances are given in Table 1, while the geometrical parameters are illustrated in Figure 2. All calculations indicated that Bp has a nonplanar structure ($\phi = 34.8\text{--}50.1^\circ$) as well as previous calculations.¹⁵ This feature also agrees well with electron diffraction experiment ($\phi = 44.4^\circ$).^{24,25} However, the calculated dihedral angles were widely distributed and those are slightly dependent on the levels of theory used in the optimizations: the twist rotation angles (ϕ) were calculated to be 50.1° (HF/3-21G(d)), 38.4° (B3LYP/6-31G(d)), and 40.5° (B3LYP/6-311G(d,p)). This distribution implies strongly that curvature of potential energy surface (PES) along the internal twist–rotation motion (ϕ direction) is very small and its shape of PES is shallow around the equilibrium point of Bp. This is due to the fact that the potential barrier for the rotation of benzene rings is significantly low. These features are in good agreement with the experimental finding that the internal twisting motion has a very low vibrational frequency of about 70 cm^{-1} in Bp.⁷

The geometrical parameters for the fully optimized structures of biphenyl cation (Bp^+) were given in Table 1. The twist angles (ϕ) were calculated to be 17.5° (HF/3-21G(d)), 19.5° (B3LYP/6-31G(d)), and 19.0° (B3LYP/6-311G(d,p)). From these values, it was concluded that structure of Bp^+ is more planar than that of neutral Bp. This is due to the fact that the electron is removed from the highest occupied molecular orbital (HOMO) of Bp. The HOMO of Bp is composed of antibonding between two benzene rings. If an electron is removed from this orbital, repulsive interaction between two rings becomes weaker, so that the Bp^+ has smaller twist angle than that of Bp.

B. Potential Energy Curves for the Internal Twist-Rotational Motion along the Twist Angle (ϕ). The potential energy curves (PECs) calculated as a function of the twist angle ϕ were plotted

TABLE 1: Optimized Geometrical Parameters for Biphenyl (Bp) and Biphenyl Cation (Bp⁺)

	Bp ^{a,b}			Bp ⁺ c		
	B3LYP/6-31G(d)	B3LYP/6-311G(d,p)	HF/3-21G(d)	B3LYP/6-31G(d)	B3LYP/6-311G(d,p)	HF/3-21G(d)
$R_{11'}^d$	1.4894	1.4858	1.4855	1.5075	1.4437	1.4422
R_{12}	1.3900	1.4053	1.4026	1.3948	1.4329	1.4306
R_{23}	1.3822	1.3941	1.3916	1.3850	1.3792	1.3759
R_{34}	1.3840	1.3961	1.3933	1.3863	1.4086	1.4057
ϕ^e	50.1	38.4	40.5	17.5	19.5	19.0

^a Experimental values for Bp (ref 24): $R_{11'}=1.509$, $R_{12}=1.406$, $R_{23}=1.397$, $R_{34}=1.398$ Å, and $\phi=44.4^\circ$. ^b Recent calculated values for Bp (ref 15): $R_{11'}=1.4840$, $R_{12}=1.4003$, $R_{23}=1.397$, $R_{34}=1.3913$ Å, and $\phi=40.1^\circ$, calculated at the B3LYP/6-311+G(2d,2p) level. ^c Recent calculated values for Bp (ref 15): $R_{11'}=1.4400$, $R_{12}=1.4281$, $R_{23}=1.3722$, $R_{34}=1.4032$ Å, and $\phi=18.9^\circ$, calculated at the B3LYP/6-311+G(2d,2p) level. ^d Bond lengths in angstroms. ^e Angles in degrees.

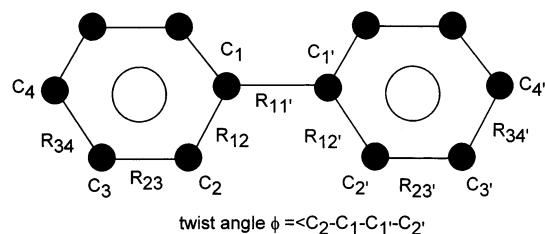


Figure 2. Geometrical parameters of biphenyl (Bp). The hydrogen atoms of Bp are omitted from this figure. Twist rotation angle is defined by ϕ .

in Figure 3. The values were calculated at the B3LYP/6-31G-(d) (Figure 3A) and HF/3-21G(d) (Figure 3B) levels of theory. The geometrical parameters except for the angle ϕ were fully optimized at each level. The symmetries of the molecule were assumed to be D_{2h} at $\phi = 0$ and D_2 at $\phi \neq 0$. For a neutral system, there are two barriers located at $\phi = 0$ and $\phi = 90^\circ$. The former and latter barriers were calculated to be 2.1 and 2.5 kcal/mol at the B3LYP/6-31G(d), respectively. The shape of potential energy curve is significantly changed at the ionized state (cation): the barrier height at $\phi = 0^\circ$ becomes lower, whereas it becomes significantly higher at $\phi = 90^\circ$. The potential minimum was located at $\phi = 20^\circ$. The potential was shallow around $\phi = 0-35^\circ$, and it becomes strongly tight at larger angles. The relative energies at $\phi = 0$ and 90° were calculated to be 0.2 and 15.6 kcal/mol, respectively.

The potential energy curves (PECs) calculated at the HF/3-21G(d) level were also plotted in Figure 3B. As clearly seen in this figure, PECs calculated by HF/3-21G(d) agreed well with those of B3LYP/6-31G(d) in lower angle regions. In both calculations, the barrier heights (relative to each minimum point) is calculated to be 0.2 kcal/mol. Thus, the HF calculations of Bp⁺ would give a reasonable feature for the potential energy curves. Therefore, we can discuss at least qualitatively the hole-capture dynamics using the results obtained by HF/3-21G(d).

C. Hole-Capture Dynamics in Biphenyl. From the static ab initio MO calculations, it was predicted that the structure of Bp is largely changed after a hole capture of Bp. In particular, the twist angle ϕ will be drastically varied as a function of time. The internal twisting mode will couple with the other internal modes of Bp⁺. Therefore, a full dimensional treatment needs to elucidate the hole-capture dynamics in Bp. In the present study, direct ab initio trajectory calculation is applied to the hole-capture process of Bp.

Figure 4 shows snapshots for the structures of Bp⁺ as a function of time after the hole capture of Bp. The snapshots of Bp⁺ at time = 0.0, 0.120, 0.260, and 0.367 ps were illustrated in Figure 4. At time zero, the twist angle was $\phi = 50.1^\circ$, which corresponds to the equilibrium structure of Bp. After a hole capture in Bp (namely, the ionization of Bp), the angle ϕ was changed gradually as a function of time. The angles at time =

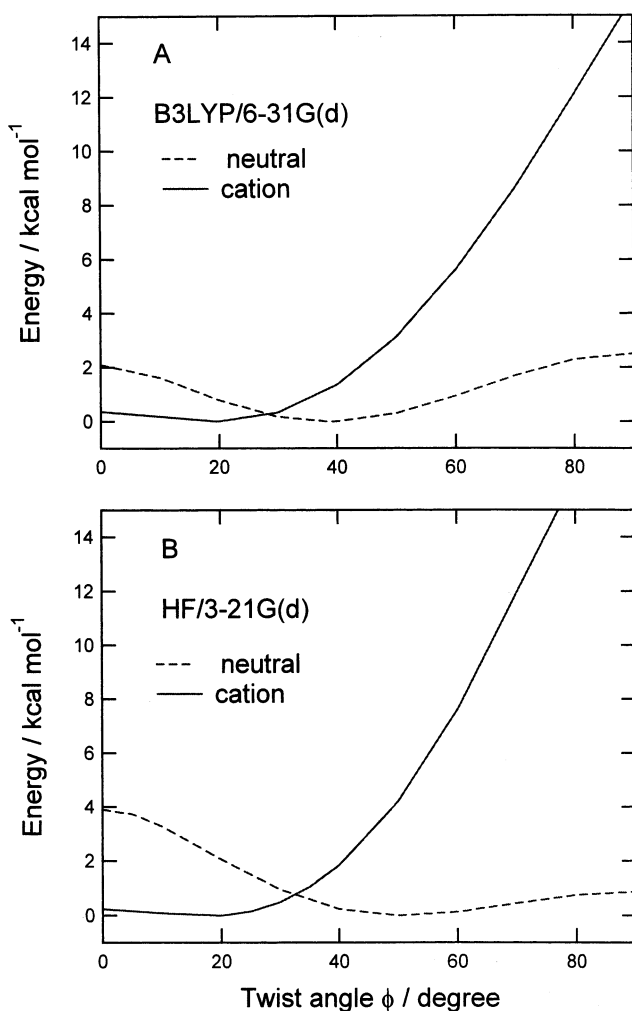


Figure 3. Potential energy curves plotted as a function of twist rotation angle (ϕ) of biphenyl (Bp) and biphenyl cation (Bp⁺). The calculations were carried out at (A) B3LYP/6-31G(d) and (B) HF/3-21G(d) levels of theory.

0.120 and 0.260 ps were calculated to be 2.3° and -45.4° , respectively. At time = 0.120 ps, the structure of Bp has a coplanar, whereas that became a twist form again at time = 0.260 ps. The twist angle was 0.0° at time = 0.367 ps, indicating that the structure of Bp⁺ is planar. Thus, the twisting motion of Bp⁺ was excited after the ionization of Bp.

To elucidate the hole-capture dynamics in more details, potential energy P , the angle ϕ , and bond distances ($R_{11'}$, R_{12} , R_{23} , and R_{34}) were plotted in Figure 5 as a function of time. The zero level of PE corresponds to the energy at vertical ionization point of Bp. After a hole capture of Bp, PE decreased suddenly to -4.8 kcal/mol, and then it further decreased gradually. PE was minimized at time = 0.198 ps (-10.8 kcal/

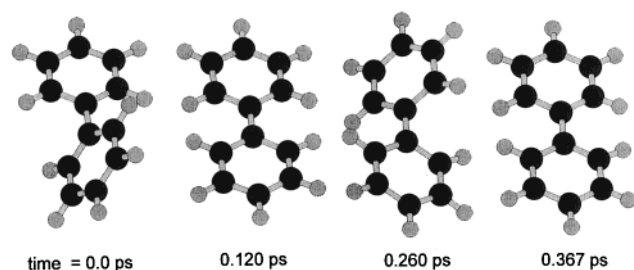


Figure 4. Snapshots for geometrical configurations of Bp^+ after vertical ionization of Bp calculated as a function of time. The direct ab initio trajectory calculation was carried out at the HF/3-21(d) level.

mol), and it vibrated with a time period of about 0.2 ps. Time dependence of twist angle was given in Figure 5B. The angle at time zero was 50.1° and it decreased gradually as a function of time. At time = 0.12 ps, the angle was close to zero, indicating that the Bp^+ ion has a planar structure. The angle was minimized at time = 0.263 ps ($\phi = -46.2^\circ$) and it reached a maximum again at time = 0.479 ps ($\phi = 45.5^\circ$). The angle vibrated with a time period of about 0.5 ps. The twist rotation motion between two benzene rings was continued because the energy of the system is not transferred into the other molecule.

The Time dependence of the C–C bond distance $R_{11'}$ is plotted in Figure 5C. The distance was 1.490 Å at time zero. After the ionization, it decreased and vibrated in the range 1.38–1.46 Å. The other C–C bond distances in the benzene ring are plotted in Figure 5D. At time zero, the distances correspond to those of Bp in the equilibrium point, which are close to each other (1.385 Å). After the hole capture, the distances were separated into three parts: in particular, R_{12} was largely elongated after the ionization.

To elucidate the initial step of the ionization process in more details, an expanded view of PE, bond distances and angles are

plotted in Figure 6. At the initial step, PE was suddenly down to -4.8 kcal/mol within 0–10 fs. The twist angles ϕ were hardly changed in this time region (0–10 fs). On the other hand, the bond distances were largely changed within 0–10 fs. For example, the C–C bond in the connection site $R_{11'}$ was rapidly shortened from 1.4897 to 1.3751 Å. The distances R_{12} , R_{23} , and R_{34} were immediately elongated. The rapid deformation is originated from Jahn–Teller effect of the Bp ring after the ionization, and it causes the rapid energy lowering of PE at 0–10 fs.

II. Hole-Capture Dynamics in Model Compound of PVB.

As shown in the previous section, the structure of Bp was changed from a nonplanar structure to a coplanar one by a hole capture. The twist angle for Bp and Bp^+ were calculated to be $\phi = 40\text{--}50^\circ$ and $15\text{--}20^\circ$, respectively. In this section, the hole-capture dynamics in PVB was investigated by means of direct PM3 trajectory calculations using a model compound composed of two-monomer units of PVB.

First, to check validity of the PM3 calculation, a trajectory of Bp^+ following the ionization of Bp was calculated by means of direct PM3 trajectory method. The results are given in Figure 7. Figure 7A shows the potential energy of the system after the ionization of Bp plotted as a function of time, while Figure 7B shows time dependence of twist rotation angle ϕ of Bp^+ . After the ionization, PE decreased to -9.3 kcal/mol and then it vibrated in the range from -9.0 to -0.8 kcal/mol. The twist angle was $\phi = 45.9^\circ$ at time zero, which is in good agreement with ab initio calculated values. The angle oscillated periodically within $\pm 40^\circ$. These features agree well with that of the ab initio calculations, suggesting that direct PM3 dynamics calculation would give a reasonable feature for the hole-capture process in the model compound of PVB. Spike of PE calculated by PM3 is larger than that of HF/3-21G(d) because the amplitude of PE calculated by the former level is slightly larger than that by

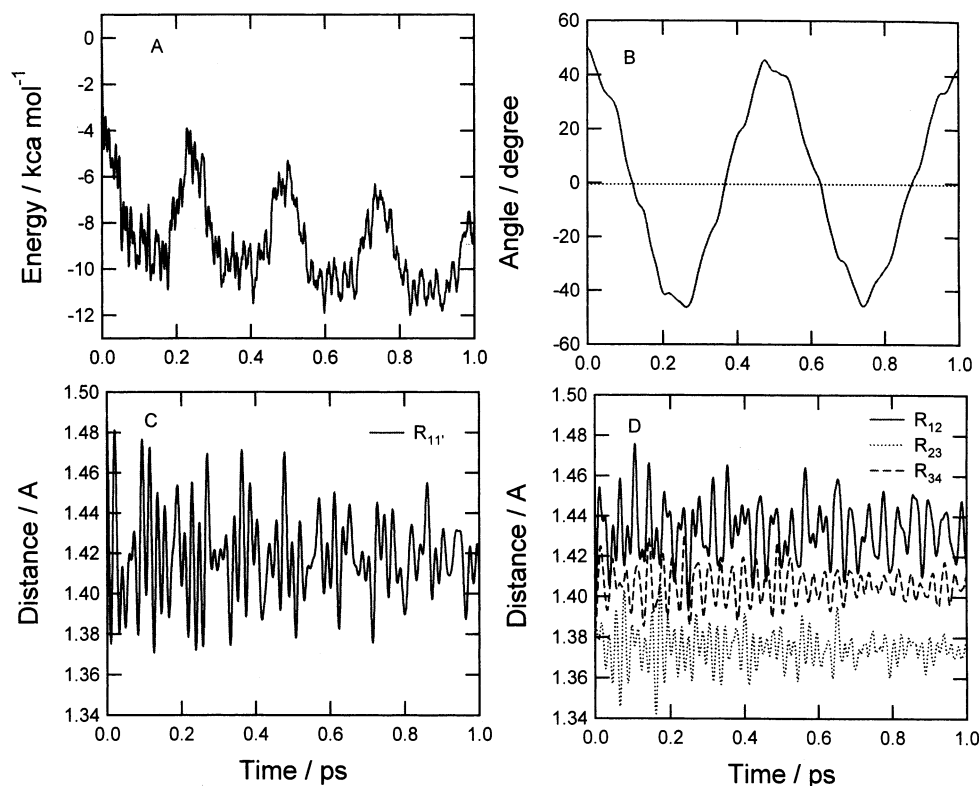


Figure 5. A trajectory of Bp^+ following the vertical ionization of Bp plotted as a function of reaction time. (A) Potential energy of the reaction system. (B) twist rotation angle ϕ . (C) Distance $R_{11'}$. (D) Distances R_{12} , R_{23} , and R_{34} versus time. The direct ab initio trajectory calculation was carried out at the HF/3-21(d) level. Snapshots are given in Figure 4.

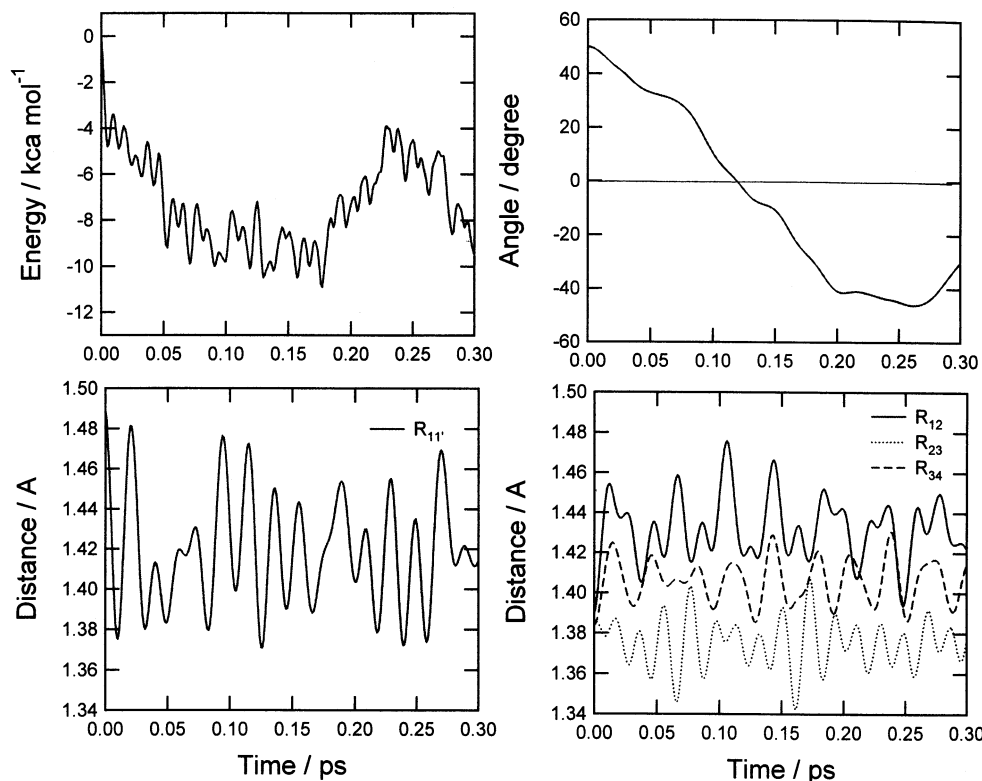


Figure 6. Expanded view of Figure 5 in short time region.

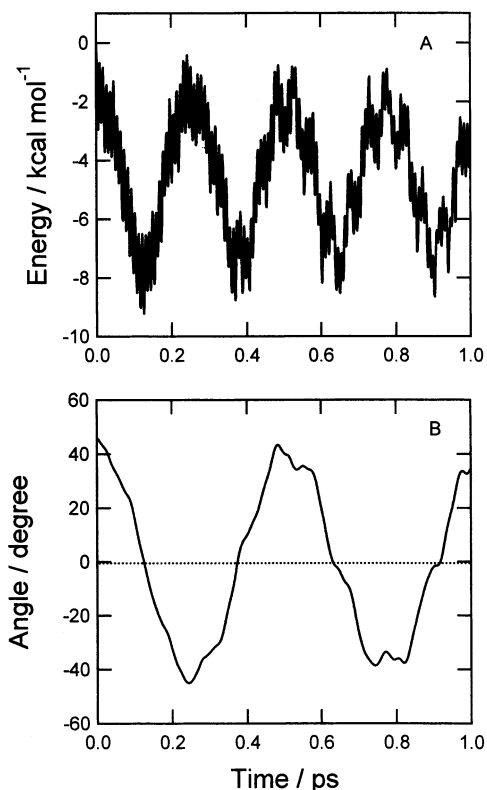


Figure 7. A trajectory of Bp^+ following the vertical ionization of Bp plotted as a function of reaction time. (A) Potential energy of the reaction system (PE). (B) Twist rotation angle ϕ . The direct trajectory calculation was carried out at the PM3 level.

latter one. The PM3 calculation would overestimate slightly the energy transfer to the internal modes.

The optimized structure of the model compound of PVB is illustrated in Figure 8 (time=0.0 in upper panel). In this model,

two monomer units of PVB were terminated by a methyl group and a hydrogen atom. The biphenyl groups for right and left position are denoted by Bp(R) and Bp(L), respectively. The structure of the model compound has no symmetry (C_1 symmetry). For neutral system of the model compound, twist angles (ϕ_R and ϕ_L) were calculated to be 45.2° and 44.2° at the PM3-MO level of theory, respectively. In both side chains, the C_1-C_1' bond distance was 1.468 \AA . The structure of Bp obtained at the PM3 level is in good agreement with the experimental and theoretical values calculated for Bp. From this structure, a trajectory was run following a vertical ionization of the model compound. The hole was first localized on Bp(R) after the ionization, and then the twist angle of $Bp^+(R)$ was rapidly changed. Two biphenyl groups $Bp^+(R)$ and Bp(L) separated from each other at time 1.0–2.0 ps because of repulsive interaction caused by a rapid deformation of twist motion. At 3.0–4.0 ps, the structure of $Bp^+(R)$ became planar and it approached Bp(L). Finally, a charge resonance state between Bp(R)–Bp(L) was formed.

Potential energy of the system PE was plotted as a function of time in Figure 8. The structure of the model compound at time zero corresponds to the optimized one. Zero level of PE corresponds to the energy of the model compound at vertical ionization. In the case of this trajectory, the hole was localized on Bp(R) at time zero. After the ionization, PE was suddenly down because the structural deformation of biphenyl ring Bp(R) was rapidly occurred, and it decreased gradually. After time = 1.0 ps, it vibrated in the range from -7 to -5 kcal/mol .

Time dependence of twist rotation angles in both biphenyl groups was plotted in Figure 8B, where ϕ_R and ϕ_L are twist rotation angles of Bp(R) and Bp(L) of the model compound, respectively. After the ionization, the angle ϕ_R was immediately changed from 45° to -28° , and then the motion vibrated with amplitude of $\pm 20^\circ$. This is due to the fact that a hole is localized on Bp(R), and the structural deformation of rings occurred (twist rotation).

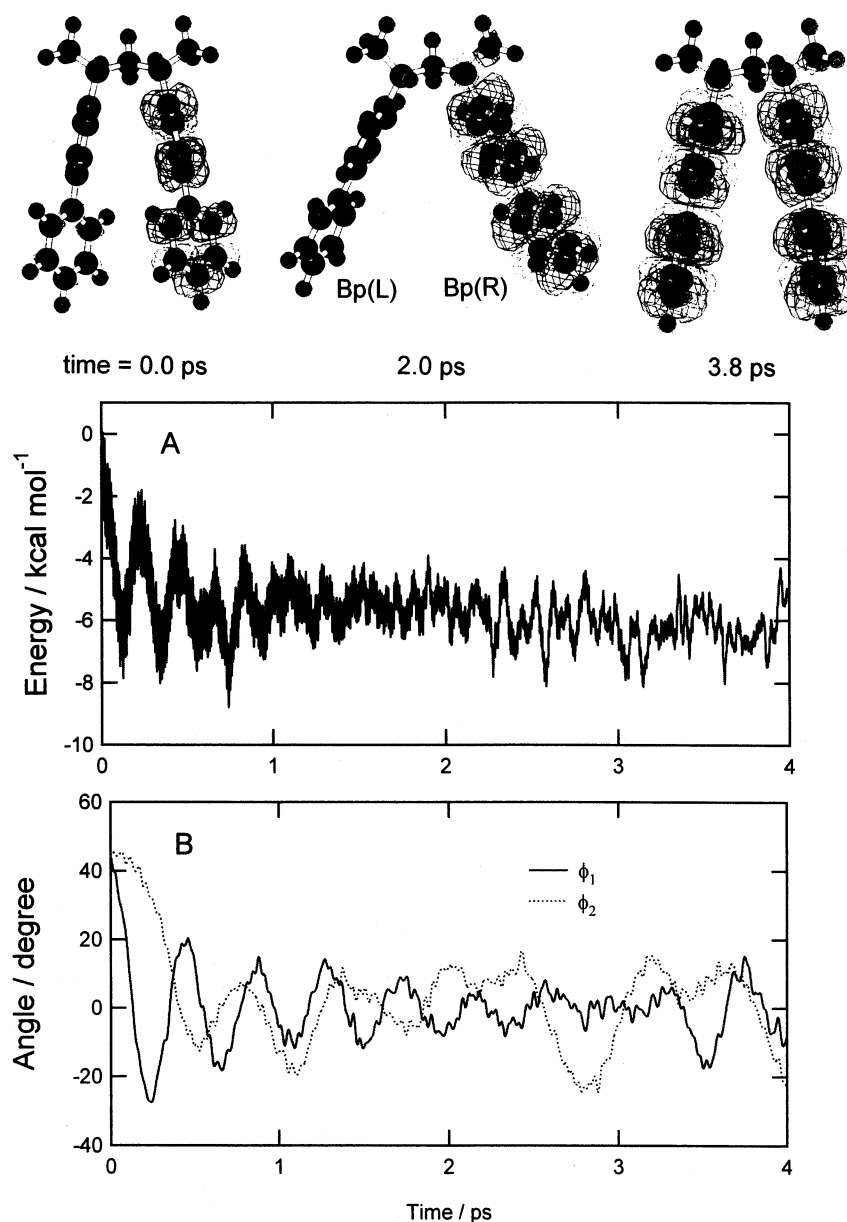


Figure 8. A trajectory of the model compound of PVB cation following the vertical ionization of neutral state. Upper illustrations: snapshots for geometrical configurations of the model compound of PVB cation and spin-orbital calculated as a function of time. (A) Potential energy of the reaction system (PE). (B) Twist rotation angles (ϕ_1 and ϕ_2) versus time. The direct trajectory calculation was carried out at the PM3 level.

As mentioned above, the ionization dynamics of the model PVB was very similar to that of Bp. The difference point is that energy relaxation process occurs efficiently in PVB because of a large bath relaxation dimension. Also, the charge resonance between Bp groups occurs in PVB.

4. Discussion

I. Dynamics of Hole Capture in Biphenyl and in PVB.

The present calculations showed that the structure of Bp is largely varied after the hole capture. In particular, twist angle ϕ is spontaneously rotated with a time period of 500 fs. Also, the C₁–C_{1'} bond distance in the connection site between the two benzene rings vibrated largely in the range 1.375–1.481 Å. The twist motion of Bp⁺ in vacuo vibrated without energy loss. The dynamics for PVB is slightly different from Bp⁺ in vacuo. The PM3 calculations using a model compound composed of a two-monomer unit of PVB showed that a hole is first localized on one of the biphenyl groups at time zero, and then it is delocalized over the two side groups.

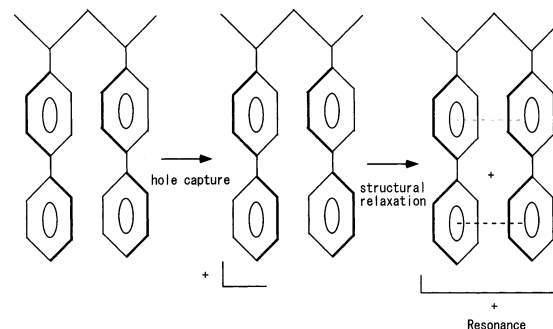


Figure 9. A model for hole capture and hole transfer in PVB.

A model of the hole-capture process of PVB, which is constructed on the basis of the present calculations, is schematically illustrated in Figure 9. After a hole capture of PVB (i.e., ionization of side-group of PVB), positive charge is localized in one of the biphenyl groups as shown in Figure 9. The biphenyl cation Bp⁺ approaches the nearest neighbor biphenyl

group possessing an internal twisting rotation, and the hole is delocalized over two biphenyl groups. If thermal energy is large enough to separate each other, charge is transferred to one of the biphenyl groups. This would be a mechanism for charge-transfer processes between neighboring side chains. The hole-hopping mechanism is also important in the case of a long-range hole transfer.

II. Comparison with Previous Studies. A recent experiment¹¹ has shown that quantum efficiency of poly(4-vinyltriphenylamine), which is a polymer with pendant triphenylamine groups in a hydrocarbon backbone, is 0.45–1.0% in the polymer, which is significantly larger than that of the devices composed of its monomer ($1.3 \times 10^{-3}\%$). The present study suggested that side chains of the polymer are easily deformed after the hole capture and then dimer of the side chains is rapidly formed. This formation would arise a large quantum efficiency in the polymer. On the other hand, monomer molecules in film orient randomly, so that hole transfer cannot take place easily. Thus, the aromatic groups in polymer, such as benzene and naphthalene, have a higher performance than the monomer crystallized in polymer film.

III. Additional Comments. We have introduced several approximations to calculate the potential energy surface and to treat the hole-capture dynamics. First, we assumed that $[\text{Bp}^+]_{\text{ver}}$ has no excess energy at the initial step of the trajectory calculation (time = 0.0 ps). This approximation may cause change of energy relaxation process of $[\text{Bp}^+]_{\text{ver}}$. Also, we assumed that initial momentum vectors of atoms are zero at time zero. However, these approximations would be adequate to treat the dynamics because the energy gradients of atoms on PES of the cation are larger than the momentum vectors of atoms, so that the effect was not considered in the present calculations. It should be noted therefore that the present model is limited in the case of no excess energy.

We assumed HF/3-21(d) and PM3 multidimensional potential energy surfaces in the trajectory calculations throughout. The shape of PES of Bp^+ at larger twist angles calculated at the HF/3-21G(d) level is slightly tighter than that of higher level calculations. Therefore, amplitude of the twist rotation mode may be slightly underestimated. On the other hand, the twist angle of Bp at the equilibrium point is calculated to be 50.1° , which is about a 5° -overestimate of the experimental value (45.0°). To check the effect of initial points of twist angle on the ionization dynamics, trajectories from several points around the equilibrium point ($\phi = 45\text{--}50^\circ$) were run for Bp^+ . The amplitude of twist rotation mode was somewhat affected by the effect of initial geometry. However, the change of amplitude was $\pm 3.0^\circ$, and the time period of the vibration was hardly changed. Therefore, this effect is negligible in order to understand the hole capture dynamics of Bp and Bp^+ . Also, as mentioned in section 3, the levels of theory represent reasonably a potential energy surface obtained by the B3LYP/6-31G* calculation. In addition, it is in good agreement with previous theoretical calculations.¹⁵ Therefore, the level of theory used in the present calculation would be adequate to discuss qualitatively the ionization dynamics of Bp. For model of PVB, we calculated the trajectory using the PM3 surface. As shown in Figures 5 and 7, the PM3 calculation reasonably represents PES of Bp^+ calculated by HF/3-21G(d). However, More accurate wave functions may provide deeper insight in the dynamics in order to gain more details feature of ionization dynamics of Bp. Such a calculation will be possible after the

development of high-speed CPU computers in the near future. Despite the several assumptions introduced here, the results enable us to obtain valuable information on the mechanism of the ionization of Bp and PVB.

Acknowledgment. The authors are indebted to the Computer Center at the Institute for Molecular Science (IMS) for the use of the computing facilities. H.T also acknowledge a partial support from a Grant-in-Aid from the Ministry of Education, Science, Sports and Culture of Japan.

References and Notes

- (1) Miller, J. R.; Paulson, P. P.; Bal, R.; Closs, G. L. *J. Phys. Chem.* **1995**, *99*, 6923.
- (2) Miller, J. R.; Beitz, J. V.; Huddleston, R. K. *J. Am. Chem. Soc.* **1984**, *106*, 5057. (b) Miller, J. R.; Calcaterra, L.; Closs, G. L. *J. Am. Chem. Soc.* **1984**, *106*, 3047. (c) Liang, N.; Miller, J. R.; Closs, G. L. *J. Am. Chem. Soc.* **1989**, *111*, 8740. (d) Liang, N.; Miller, J. R.; Closs, G. L. *J. Am. Chem. Soc.* **1990**, *112*, 5353. Closs, G. L.; Calcaterra, L. T.; Green, N. J.; Penfield, K. W.; Miller, J. R. *J. Phys. Chem.* **1986**, *90*, 3673. (f) Closs, G. L.; Miller, J. R. *Science* **1988**, *240*, 440.
- (3) Chen, E. C. M.; Wentworth, W. E. *Mol. Cryst. Liq. Cryst.* **1989**, *171*, 271.
- (4) Ruscic, B.; Kovac, B.; Klasinc, L.; Gusten, H. Z. *Naturforsch* **1978**, *33A*, 1006.
- (5) Bastiansen, O. *Acta Chem. Scand.* **1949**, *3*, 408.
- (6) Bastiansen, O.; Samdal, S. *J. Mol. Struct.* **1985**, *128*, 115.
- (7) Tsuzuki, Y.; Tanabe, K. *J. Phys. Chem.* **1991**, *95*, 139.
- (8) Takei, Y.; Yamaguchi, T.; Osamura, Y.; Fuke, K.; Kaya, K. *J. Phys. Chem.* **1988**, *92*, 577.
- (9) Buntinx, G.; Poizat, O. *J. Chem. Phys.* **1989**, *91*, 2153.
- (10) Ogasawara, M. *Radiat. Phys. Chem.* **1997**, *49*, 71.
- (11) Feast, W. J.; Peace, R. J.; Sage, I. C.; Wood, E. L. *Polym. Bull.* **1999**, *42*, 167.
- (12) Bellmann, E.; Shaheen, S. E.; Thayumanavan, S.; Barlow, S.; Grubbs, R. H.; Marder, S. R.; Kippelen, B.; Peyghambarian, N. *Chem. Mater.* **1998**, *10*, 1668.
- (13) Dodabalarpur, A. *Solid State Commun.* **1997**, *102*, 259.
- (14) Itano, K.; Ogawa, H.; Shiota, Y. *Appl. Phys. Lett.* **1998**, *65*, 807.
- (15) Arulmozhiraja, S.; Fujii, T. *J. Chem. Phys.* **2001**, *115*, 10589.
- (16) (a) Rubio, M.; Merchan, M.; Orti, E.; Roos, B. O. *J. Phys. Chem.* **1995**, *99*, 14980. (b) Merchan, M.; Serrano-Andres, L.; Gonzales-Luque, R.; Roos, B. O.; Rubio, M. *J. Mol. Struct. (THEOCHEM)* **1999**, *463*, 201.
- (17) (a) Vreven, T.; Bernardi, F.; Garavelli, M.; Olivucci, M.; Robb, M. A.; Schlegel, H. B. *J. Am. Chem. Soc.* **1997**, *119*, 12687. (b) Chen, W.; Hase, W. L.; Schlegel, H. B. *Chem. Phys. Lett.* **1994**, *228*, 436. (c) Li, G. S.; Hase, W. L. *J. Am. Chem. Soc.* **1999**, *121*, 7124. Helgaker, E.; Uggerud, H.; Jonsen, H. J. A. *Chem. Phys. Lett.* **1990**, *173*, 145. Tachikawa, H. *Chem. Phys.* **2001**, *273*, 149.
- (18) Karplus, M.; Porter, R. N.; Sharma, R. D. *J. Chem. Phys.* **1965**, *43*, 3259.
- (19) (a) Tachikawa, H. *J. Chem. Phys.* **1998**, *108*, 3866. (b) Tachikawa, H. *J. Phys. B*, **1999**, *32*, 1451.
- (20) (a) H. Tachikawa, *J. Phys. Chem. A* **2001**, *105*, 1260. (b) H. Tachikawa, *J. Phys. Chem. A* **2000**, *104*, 497.
- (21) (a) Tachikawa, H. *Phys. Chem. Chem. Phys.* **2000**, *2*, 839. (b) Tachikawa, H. *Phys. Chem. Chem. Phys.* **2000**, *2*, 4702.
- (22) Program code of the direct ab initio trajectory calculation was created by our group.
- (23) Ab initio MO program, see: Frisch, M. J.; Trucks, G. W.; Schlegel, H. B.; Scuseria, G. E.; Robb, M. A.; Cheeseman, J. R.; Zakrzewski, V. G.; Montgomery, J. A., Jr.; Stratmann, R. E.; Burant, J. C.; Dapprich, S.; Millam, J. M.; Daniels, A. D.; Kudin, K. N.; Strain, M. C.; Farkas, O.; Tomasi, J.; Barone, V.; Cossi, M.; Cammi, R.; Mennucci, B.; Pomelli, C.; Adamo, C.; Clifford, S.; Ochterski, J.; Petersson, G. A.; Ayala, P. Y.; Cui, Q.; Morokuma, K.; Malick, D. K.; Rabuck, A. D.; Raghavachari, K.; Foresman, J. B.; Cioslowski, J.; Ortiz, J. V.; Stefanov, B. B.; Liu, G.; Liashenko, A.; Piskorz, P.; Komaromi, I.; Gomperts, R.; Martin, R. L.; Fox, D. J.; Keith, T.; Al-Laham, M. A.; Peng, C. Y.; Nanayakkara, A.; Gonzalez, C.; Challacombe, M.; Gill, P. M. W.; Johnson, B. G.; Chen, W.; Wong, M. W.; Andres, J. L.; Head-Gordon, M.; Replogle, E. S.; Pople, J. A. *Gaussian 98*, revision A.5; Gaussian, Inc.: Pittsburgh, PA, 1998.
- (24) Almenningen, A.; Bastiansen, O.; Fernholt, F.; Cyvin, B. N.; Cyvin, S. J.; Samdal, S. *J. Mol. Struct.* **1985**, *128*, 59.
- (25) Bastiansen, O.; Samdal, S. *J. Mol. Struct.* **1985**, *128*, 115.